Scientific Research Publishing

Journal of Modern Physics, 2023, 14, 1741-1754
https://www.scirp.org/journal/jmp
ISSN Online: 2153-120X
ISSN Print: 2153-1196

Understanding the Formation of Galaxies with Warm Dark Matter

Bruce Hoeneisen

Universidad San Francisco de Quito, Quito, Ecuador
Email: bhoeneisen@usfq.edu.ec

How to cite this paper: Hoeneisen, B. (2023) Understanding the Formation of Galaxies with Warm Dark Matter. *Journal of Modern Physics*, **14**, 1741-1754.
https://doi.org/10.4236/jmp.2023.1413103

Received: October 9, 2023
Accepted: December 19, 2023
Published: December 22, 2023

Abstract

The formation of galaxies with warm dark matter is approximately adiabatic. The cold dark matter limit is singular and requires relaxation. In these lecture notes, we develop, step-by-step, the physics of galaxies with warm dark matter, and their formation. The theory is validated with observed spiral galaxy rotation curves. These observations constrain the properties of the dark matter particles.

Keywords

Warm Dark Matter, Galaxy, Galaxy Formation

1. Introduction

The formation of galaxies is qualitatively different if dark matter is warm instead of cold. The cold dark matter limit is singular. It turns out that understanding galaxies, and the formation of galaxies, is *less difficult* if dark matter is warm. So we add to the cold dark matter ΛCDM cosmology one more parameter, namely the temperature-to-mass ratio of dark matter, and let observations decide whether dark matter is warm or cold. These lecture notes do bring new understanding of dark matter, and constrain the properties of the dark matter particles.

There is an extensive literature on warm dark matter, e.g. [1] and references therein. Here, our main focus of attention is the understanding of a relation between observables and an adiabatic invariant in the early universe, which is either an unlikely coincidence, or the solution to the long-standing dark matter problem.

2. Warm Dark Matter

Let us consider warm dark matter as a non-relativistic classical noble gas of par-

ticles of mass m, density ρ and temperature T. By "classical" we mean that the velocity distribution of the non-relativistic particles of dark matter in the early universe is assumed to be the Maxwell distribution, *i.e.* is not degenerate. For a discussion on how dark matter might have acquired the Maxwell distribution of velocities, see [2]. By "noble" we mean that collisions, if any, do not excite internal states of the particles. Recall that for a non-relativistic gas, $\frac{1}{2}m\langle v^2\rangle = \frac{3}{2}kT$. $\sqrt{\langle v^2\rangle}$ is the root-mean-square thermal velocity of the dark matter particles. Recall that for adiabatic expansion of a noble gas, $TV^{\gamma-1} = TV^{2/3} = \text{constant}$ (here V is the volume), so

$$\sqrt{\langle v^2\rangle}\,\rho^{-1/3} = \text{constant} \tag{1}$$

is an adiabatic invariant. We will review these concepts in more detail in the next lecture. We want to stress that Equation (1) is valid for a collisionless or collisional gas, and is valid whether, or not, the particles are bouncing off the walls of an expanding box of volume V.

To verify these statements, let us now consider a free particle in a homogeneous universe with expansion parameter $a(t)$, normalized to $a(t_0)=1$ at the present time t_0. The particle has velocity v at the space point $\boldsymbol{r}$. In time $\mathrm{d}t$ the particle advances $v\mathrm{d}t$ and arrives at the space point $\boldsymbol{r}'$. Due to the expansion of the universe, $\boldsymbol{r}'$ moves away from $\boldsymbol{r}$ with velocity

$$Hv\mathrm{d}t = \frac{1}{a}\frac{\mathrm{d}a}{\mathrm{d}t}v\mathrm{d}t = \frac{\mathrm{d}a}{a}v. \tag{2}$$

So the velocity of the free particle relative to $\boldsymbol{r}'$, when it coincides with $\boldsymbol{r}'$, is reduced by $-\mathrm{d}v = (\mathrm{d}a/a)v$, so

$$va = \text{constant}. \tag{3}$$

Note that this expression is in agreement with Equation (1). As the universe expands, velocities decrease in proportion to a^{-1}, the temperature decreases in proportion to a^{-2}, and the density decreases in proportion to a^{-3}.

It is not necessary to invoke General Relativity. The preceding arguments are valid also in the non-relativistic physics of Newton. During galaxy formation, the dark matter particles have a velocity field in addition to the thermal velocity. Whenever the velocity field diverges, dark matter cools as described in the preceding paragraph.

We define the "adiabatic invariant" of warm dark matter as the comoving root-mean-square thermal velocity of the dark matter particles:

$$v_{h\mathrm{rms}}(1) \equiv v_{h\mathrm{rms}}(a)a = v_{h\mathrm{rms}}(a)\left(\frac{\Omega_c\rho_{\mathrm{crit}}}{\rho_h(a)}\right)^{1/3}. \tag{4}$$

$\Omega_c\rho_{\mathrm{crit}}$ is the mean dark matter density of the universe at the present time (throughout we use the notation and the values of parameters of [3]). The sub-index h stands for the dark matter halo. We will use the sub-index b for "baryons", mostly hydrogen and helium. These sub-indices will be used only

when needed.

Consider a free observer in a density peak in the early universe. This observer feels no gravity and "sees" warm dark matter expand adiabatically, reach maximum expansion, and then contract adiabatically into the core of a galaxy. The adiabatic invariant (4) in the early universe remains constant in the core of the galaxy throughout the formation of the galaxy. This statement is non-trivial, so we will study it in detail in the following lectures, and finally will validate it with observations.

To the cold dark matter cosmology ΛCDM, that has six parameters [3], we add one more parameter, namely the adiabatic invariant $v_{hrms}(1)$, and obtain the warm dark matter cosmology ΛWDM. As we shall learn in the following lectures, we are able to measure v_{hrms} and ρ_{0h} in the core of spiral galaxies, and will therefore be able to obtain $v_{hrms}(1)$, and then decide whether dark matter is warm or cold.

3. The Exponential Isothermal Atmosphere

This lecture is included to remind the reader of results we will be using later on. (For more background, I recommend studying the awe inspiring Feynman Lectures on "The exponential atmosphere" [4].)

James Clerk Maxwell presented several clever arguments to obtain the distribution of velocities of the particles in a gas in thermal equilibrium. The number of particles per unit phase space volume $\mathrm{d}^3\boldsymbol{r}\mathrm{d}^3\boldsymbol{p} \equiv \mathrm{d}x\mathrm{d}y\mathrm{d}z\mathrm{d}p_x\mathrm{d}p_y\mathrm{d}p_z$ is proportional to $\exp\left[-p^2/(2mkT)\right]$:

$$\frac{\mathrm{d}n}{\mathrm{d}^3\boldsymbol{r}\mathrm{d}^3\boldsymbol{p}} \propto \exp\left[-\frac{p^2}{2mkT}\right], \tag{5}$$

where $\boldsymbol{p} = m\boldsymbol{v}$ is the particle momentum. The momenta $\boldsymbol{p}$ are assumed isotropic (later on we will lift this assumption when needed). This Maxwell distribution has been validated experimentally (which settles the issues of the clever arguments), and is our point of departure in these lectures. Using the definite integrals

$$\int_0^\infty \mathrm{e}^{-x^2}x^2\mathrm{d}x = \frac{\sqrt{\pi}}{4}, \quad \int_0^\infty \mathrm{e}^{-x^2}x^4\mathrm{d}x = \frac{3\sqrt{\pi}}{8}, \tag{6}$$

the following well known results are readily obtained:

$$\frac{1}{2}m\left\langle v^2\right\rangle = \frac{3}{2}kT, \quad P = \frac{\rho}{m}kT \quad \text{with } \rho \equiv \frac{N}{V}m, \tag{7}$$

where the pressure P is defined as twice the momenta p_z of particles with $p_z > 0$ traversing unit area in unit time.

Let N/V be the number of particles per unit volume of the gas. Then the normalized Maxwell distribution is

$$\frac{\mathrm{d}n}{\mathrm{d}^3\boldsymbol{r}\mathrm{d}^3\boldsymbol{p}} = \frac{N}{V}\frac{1}{(2\pi mkT)^{3/2}}\exp\left[\frac{-p^2}{2mkT}\right]. \tag{8}$$

The number of particles with z-momenta in the interval p_z to $p_z + \mathrm{d}p_z$, traversing unit area in unit time, obtained from (8), is

$$\mathrm{d}F = v_z \mathrm{d}p_z \int \frac{N}{V} \frac{1}{\left(2\pi mkT\right)^{3/2}} \exp\left[\frac{-p^2}{2mkT}\right] \mathrm{d}p_x \mathrm{d}p_y. \tag{9}$$

Now consider gas in equilibrium in a column in a uniform gravitational field $\boldsymbol{g} = g_z \boldsymbol{e}_z$ with $g_z < 0$. The potential energy of a particle at altitude $z = h$ is $\Phi(h) = m(-g_z)h$. We wish to obtain the distribution of momenta at altitude h. We consider particles at altitude 0 with $p_z > 0$ and $p_z^2/(2m) > \Phi(h)$, with z-momenta in the interval p_z to $p_z + \mathrm{d}p_z$. These particles reach altitude h with z-momenta in the interval p_z' to $p_z' + \mathrm{d}p_z'$, where

$$\frac{p_z^2}{2m} = \frac{p_z'^2}{2m} + \Phi(h) \quad \text{and} \quad \frac{\left(p_z + \mathrm{d}p_z\right)^2}{2m} = \frac{\left(p_z' + \mathrm{d}p_z'\right)^2}{2m} + \Phi(h). \tag{10}$$

Subtracting these two equations, and keeping first order terms, obtains

$$v_z \mathrm{d}p_z = v_z' \mathrm{d}p_z'. \tag{11}$$

Multiplying by $\mathrm{d}t$ obtains

$$\mathrm{d}z\mathrm{d}p_z = \mathrm{d}z'\mathrm{d}p_z'. \tag{12}$$

This equation is Liouville's theorem in one dimension: the volume of phase space occupied by a set of particles moving in a conservative field is a constant of the motion.

In the steady state, the flux $\mathrm{d}F'$ of particles at altitude h with z-momenta in the interval p_z' to $p_z' + \mathrm{d}p_z'$ is the same as the flux $\mathrm{d}F$ of particles at altitude 0 with z-momenta in the interval p_z to $p_z + \mathrm{d}p_z$, since these are the same particles. Therefore, expressing $\mathrm{d}F$ in terms of variables at altitude h, we obtain:

$$\mathrm{d}F = \mathrm{d}F' = v_z' \mathrm{d}p_z' \int \left(\frac{N}{V}\right)' \frac{1}{\left(2\pi mkT\right)^{3/2}} \exp\left[\frac{-p'^2}{2mkT}\right] \mathrm{d}p_x' \mathrm{d}p_y'. \tag{13}$$

where

$$\left(\frac{N}{V}\right)' = \frac{N}{V} \exp\left[\frac{-\Phi(h)}{kT}\right] \tag{14}$$

So, the density varies with altitude as

$$\rho(h) = \rho(0) \exp\left[\frac{-\Phi(h)}{kT}\right]. \tag{15}$$

Comparing (13) with (9), we obtain the distribution of particles at any altitude:

$$\frac{\mathrm{d}n}{\mathrm{d}^3\boldsymbol{r}\mathrm{d}^3\boldsymbol{p}} \propto \exp\left[-\frac{E}{kT}\right], \tag{16}$$

where the energy of a particle is

$$E = \frac{p^2}{2m} + \Phi(\boldsymbol{r}). \tag{17}$$

Equation (16) is the Boltzmann distribution. The proportionality constant in (16) is independent of altitude. Note that T in (16) is the same T as in (8), so the column of gas is isothermal! These equations are valid for general potential energies $\Phi(\boldsymbol{r})$ not explicitly dependent on *t*.

An amazing result of these calculations is that the root-mean-square velocity $\sqrt{\langle v^2 \rangle}$ of the particles of the gas is independent of altitude! This is because only the more energetic particles with the Maxwell distribution reach a higher altitude. Another amazing result is that the column of gas is isothermal because of the Maxwell distribution of momenta, not because of thermal contact, or not, with the walls (if any) of the gas column.

We have not considered particle collisions. It turns out that results are unchanged because collisions conserve energy (another non-trivial statement).

If the particles are collisionless, the thermal velocities may not be isotropic, in which case we will consider separately each component of the thermal velocity.

One more equation that we will be using in the sequel is

$$\frac{\mathrm{d}P}{\mathrm{d}z} = \frac{mg_z}{kT} P = \rho g_z, \tag{18}$$

in agreement with (15). This equation expresses that the difference of pressure $P(z) - P(z+\mathrm{d}z)$ supports the weight of the gas between z and $z+\mathrm{d}z$. This result may again be surprising since there are no membranes at z and $z+\mathrm{d}z$ on which the particles can bounce off. Equation (18) expresses conservation of momentum.

4. The Cored Isothermal Sphere

Let us repeat the arguments of the preceding lecture, but this time we consider a self-gravitating gas with spherical symmetry. The equations to be solved are

$$\nabla \cdot \boldsymbol{g} = \frac{1}{r^2}\frac{\mathrm{d}}{\mathrm{d}r}\left(r^2 g_r\right) = -4\pi G\rho, \quad \nabla P = \frac{\mathrm{d}P}{\mathrm{d}r}\boldsymbol{e}_r = \rho \boldsymbol{g}, \quad P = \left\langle v_r^2 \right\rangle \rho. \tag{19}$$

The rotation velocity $V(r)$ of a test particle in a circular orbit of radius r is given by

$$-g_r(r) = \frac{V(r)^2}{r}. \tag{20}$$

First we seek a particular solution of the form $\rho(r) \propto r^n$, with $\left\langle v_r^2 \right\rangle$ independent of r, *i.e.* we limit the scope of the present lectures to the isothermal case. There is a single well known solution of this form (with $n = -2$):

$$\rho(r) = \frac{kT}{2\pi G m r^2}, \quad M(r) = \frac{2kT}{Gm} r, \quad V = \sqrt{\frac{2kT}{m}} = \sqrt{2\left\langle v_r^2 \right\rangle}. \tag{21}$$

The potential energy difference between particles at r and a reference r_c is $\Phi(r) = 2kT \ln(r/r_c)$, so (15) is valid. Note that to obtain a solution it is necessary to provide $\left\langle v_r^2 \right\rangle$.

The total mass of the halo can be defined as $M(r_{\max})$ with $\rho(r_{\max}) = \Omega_c \rho_{\mathrm{crit}}$. Then $M(r_{\max}) \propto T^{3/2} \propto V^3$, which is the Tully-Fisher relation if $M(r_{\max})$ is

proportional to the absolute luminosity.

Let us review Liouville's theorem for the problem at hand. Let $\mathrm{d}n$ be the number of particles occupying the phase-space volume $\mathrm{d}^3\boldsymbol{r}\mathrm{d}^3\boldsymbol{p}$. If the force field is conservative, *i.e.* if (17) is satisfied with $\Phi(\boldsymbol{r})$ not explicitly dependent on t, then, in the course of the motion of the $\mathrm{d}n$ particles, the corresponding volume of phase-space moves in phase-space, and may change shape, but its volume turns out to be a constant of the motion. Also, no particles cross the boundary of this phase-space volume, so $\mathrm{d}n$ is also a constant of the motion. The phase-space density $\left(\mathrm{d}n/\left(\mathrm{d}^3\boldsymbol{r}\mathrm{d}^3\boldsymbol{p}\right)\right)$ at time t is equal to the phase-space density $\left(\mathrm{d}n/\left(\mathrm{d}^3\boldsymbol{r}\mathrm{d}^3\boldsymbol{p}\right)\right)'$ at time t', and so can only be a function of constants of the motion, e.g. the energy E. If this function of E is exponential the system is isothermal, *i.e.* $\langle v^2\rangle$ is independent of $\boldsymbol{r}$. In the present case of the isothermal sphere, E does not depend on the directions of $\boldsymbol{r}$ or $\boldsymbol{p}$, so the phase-space volume can be written as $4\pi r^2\mathrm{d}r\cdot 4\pi p^2\mathrm{d}p$, with $\boldsymbol{v}\cdot\mathrm{d}\boldsymbol{p}=\boldsymbol{v}'\cdot\mathrm{d}\boldsymbol{p}'$, and, in particular, $v_r\mathrm{d}p_r=v_r'\mathrm{d}p_r'$. If convenient, the phase-space volume can also be written as $4\pi r^2\mathrm{d}r\cdot\mathrm{d}p_r\cdot 2\pi p_T\mathrm{d}p_T$, where $\boldsymbol{p}_T$ is the momentum transverse to $\boldsymbol{e}_r$. Then the flux at r per unit area and time of particles with p_r in $\mathrm{d}p_r$, and similarly at r', are

$$\mathrm{d}F\equiv\frac{\mathrm{d}n}{4\pi r^2\mathrm{d}t}=v_r\mathrm{d}p_r\int\left(\frac{\mathrm{d}n}{\mathrm{d}^3\boldsymbol{r}\mathrm{d}^3\boldsymbol{p}}\right)2\pi p_T\mathrm{d}p_T,\tag{22}$$

$$\mathrm{d}F'\equiv\frac{\mathrm{d}n}{4\pi r'^2\mathrm{d}t'}=v_r'\mathrm{d}p_r'\int\left(\frac{\mathrm{d}n}{\mathrm{d}^3\boldsymbol{r}\mathrm{d}^3\boldsymbol{p}}\right)'2\pi p_T'\mathrm{d}p_T',\tag{23}$$

Note that $\mathrm{d}t\equiv\mathrm{d}r/v_r=\mathrm{d}r'/v_r'\equiv\mathrm{d}t'$, so $4\pi r^2\mathrm{d}F=4\pi r'^2\mathrm{d}F'$.

Equations (19) can be solved numerically in radial steps $\mathrm{d}r$, starting from $r_{\min}$. To start the numerical integration we need to provide two boundary conditions, e.g. $g_r(r_{\min})$ and $\rho(r_{\min})$, in addition to $\langle v_r^2\rangle$. For solutions with no black hole at $r=0$ we can take $g_r(r_{\min})\approx -G4\pi r_{\min}\rho(r_{\min})/3$. For these isothermal spheres with a core the solution for $r\gg r_c$ is (21), while the solution for $r\ll r_c$ is

$$\rho(r\ll r_c)=\rho_0,\quad V(r\ll r_c)=\sqrt{\frac{4}{3}\pi G\rho_0}\,r,\quad \Phi(r\ll r_c)\equiv 0.\tag{24}$$

The two asymptotes meet at a "core radius"

$$r_c=\sqrt{\frac{3\langle v_r^2\rangle}{2\pi G\rho_0}}.\tag{25}$$

We note that the adiabatic invariant (1) is a minimum at $r=0$ where $\Phi(r)$ is a minimum. Since the cored isothermal sphere has formed from a density perturbation in the early universe, its two parameters ρ_0 and $\langle v_r^2\rangle=kT/m$ are related by the adiabatic invariant (4):

$$v_{hrms}(1)=\sqrt{3\langle v_r^2\rangle}\left(\frac{\Omega_c\rho_{\mathrm{crit}}}{\rho_0}\right)^{1/3}.\tag{26}$$

Further justification of (26), and observational validation, will be given in following lectures. Therefore, in the present work, the cored isothermal sphere, and its Boltzmann distribution of dark matter particles, is defined by a single independent parameter, ρ_0 or $\langle v_r^2 \rangle = kT/m$. Equation (26) assumes isotropic velocities (valid in the core due to spherical symmetry, and also valid if the dark matter halo is isothermal).

We note that a measurement of $V(r \gg r_c)$ obtains $\sqrt{\langle v_r^2 \rangle}$, and a measurement of $\mathrm{d}V(r \ll r_c)/\mathrm{d}r$ obtains ρ_0, and together they obtain the adiabatic invariant $v_{hrms}(1)$.

5. An Example

As an extreme example, with a very large ρ_{0h}, let us consider the spiral galaxy UGC11914 (note that our final measurements of $v_{hrms}(1)$ are obtained from rotation curves of dwarf galaxies [6]). The rotation curves of UGC11914, observed by the SPARC collaboration [5], are presented in **Figure 1**. We fit these rotation curves by solving the equations:

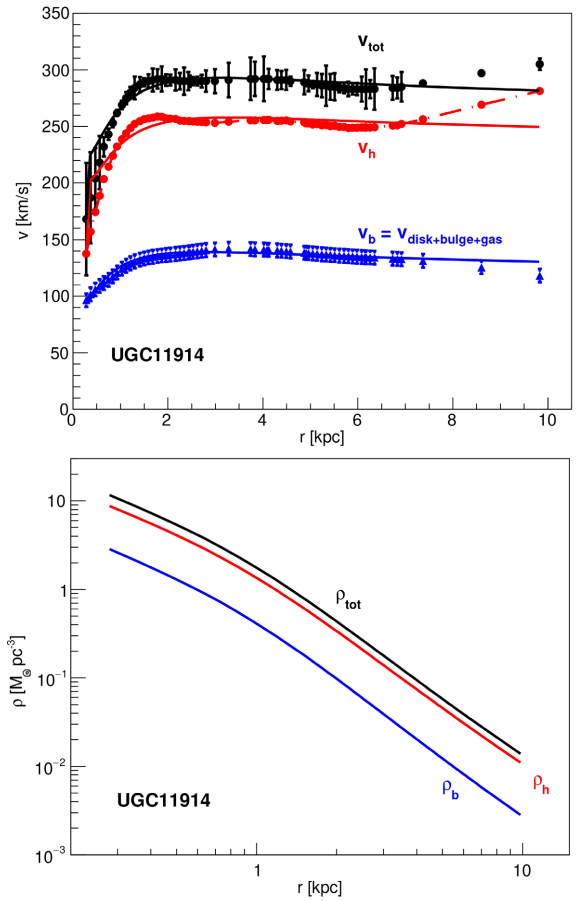

Figure 1. Top: Observed rotation curve $V_{\mathrm{tot}}(r)$ (dots) and the baryon contribution $V_b(r)$ (triangles) of galaxy UGC11914 [5]. The solid lines are obtained by numerical integration as explained in the text. Bottom: Mass densities of baryons and dark matter obtained by the numerical integration.

$$\nabla \cdot \boldsymbol{g}_b = -4\pi G\rho_b, \quad \nabla \cdot \boldsymbol{g}_h = -4\pi G\rho_h, \tag{27}$$

$$\boldsymbol{g} = \boldsymbol{g}_b + \boldsymbol{g}_h, \quad g_b \equiv -\frac{v_b^2}{r}, \quad g_h \equiv -\frac{v_h^2}{r}, \quad V^2 = v_b^2 + v_h^2, \tag{28}$$

$$\nabla P_b = \rho_b\left(\boldsymbol{g} + \kappa_b \frac{V^2}{r}\hat{\boldsymbol{e}}_r\right), \quad \nabla P_h = \rho_h\left(\boldsymbol{g} + \kappa_h \frac{V^2}{r}\hat{\boldsymbol{e}}_r\right), \tag{29}$$

$$P_b = \left\langle v_{rb}^2 \right\rangle \rho_b \quad \text{and} \quad P_h = \left\langle v_{rh}^2 \right\rangle \rho_h. \tag{30}$$

$\boldsymbol{g}_b$ and $\boldsymbol{g}_h$ are the contributions of baryons and dark matter to the gravitation field $\boldsymbol{g}$. We have included κ_b and κ_h to account for rotation. These parameters are quite uncertain, though a rough estimate is $\kappa_b \approx 0.98$ and $\kappa_h \approx 0.15$ [7] or less [8]. We can eliminate κ_b and κ_h from the numerical integration by replacing $\left\langle v_{rb}^2 \right\rangle \to \left\langle v_{rb}^2 \right\rangle / (1-\kappa_b)$, and $\left\langle v_{rh}^2 \right\rangle \to \left\langle v_{rh}^2 \right\rangle / (1-\kappa_h)$. We start the numerical integration at the first measured point at $r_{\min}$, and end at the last measured point, in steps dr. To start the numerical integration we need six boundary conditions: $\left\langle v_{rb}^2 \right\rangle / (1-\kappa_b)$, $\left\langle v_{rh}^2 \right\rangle / (1-\kappa_h)$, $\rho_b(r_{\min})$, $\rho_h(r_{\min})$, M_{bBH} and M_{hBH}, where

$$g_b(r_{\min}) = -G(4/3)\pi r_{\min}\rho_b(r_{\min}) - GM_{bBH}/r_{\min}^2, \tag{31}$$

$$g_h(r_{\min}) = -G(4/3)\pi r_{\min}\rho_h(r_{\min}) - GM_{hBH}/r_{\min}^2, \tag{32}$$

to include the possibility of a black hole at the center. Good fits are obtained assuming $\left\langle v_{rb}^2 \right\rangle / (1-\kappa_b)$ and $\left\langle v_{rh}^2 \right\rangle / (1-\kappa_h)$ are independent of r. We vary the six boundary conditions to minimize the χ^2 between the observed and calculated rotation velocities, and obtain:

$$\sqrt{\frac{\left\langle v_{rb}^2 \right\rangle}{1-\kappa_b}} = 193.9 \pm 1.7 \text{ km/s}, \quad \sqrt{\frac{\left\langle v_{rh}^2 \right\rangle}{1-\kappa_h}} = 197.5 \pm 0.8 \text{ km/s}, \tag{33}$$

$$\rho_b(r_{\min}) = 2.86 \pm 0.22 \text{ M}_\odot/\text{pc}^3, \quad \rho_h(r_{\min}) = 8.75 \pm 0.29 \text{ M}_\odot/\text{pc}^3, \tag{34}$$

$$M_{bBH} = (2.85 \pm 0.95) \times 10^8 \text{ M}_\odot, \quad M_{hBH} = (18.6 \pm 2.0) \times 10^8 \text{ M}_\odot. \tag{35}$$

Uncertainties are statistical from the fit. The core radius is 0.70 kpc. The core dark matter density $\rho_h(r_{\min})$ is 2.6 × 10^8 times the mean dark matter density of the universe $\Omega_c \rho_{\text{crit}}$. We note that this galaxy indeed has a black hole at its center. From $\left\langle v_{rh}^2 \right\rangle$ and $\rho_h(r_{\min})$ we obtain the adiabatic invariant (26):

$$v_{h\text{rms}}(1) = \sqrt{1-\kappa_h} \cdot (535 \pm 8(\text{stat}))\text{m/s}, \tag{36}$$

where the uncertainty is statistical only.

Let us mention that similar results are obtained from galaxies spanning 3.5 orders of magnitude in absolute luminosity [6], validating that the adiabatic invariant in the core of galaxies is conserved, confirming that $v_{h\text{rms}}(1)$ is of cosmological origin, and that dark matter is indeed warm!

If we add an r-dependence to $\left\langle v_{rh}^2 \right\rangle$ we generally obtain a higher χ^2 of the fit, so indeed, within uncertainties, the dark matter halo is isothermal, at least out to the observed rotation curves, indicating that the particles have the Max-

well-Boltzmann momentum distribution. We note that $\sqrt{\langle v_{rb}^2\rangle/(1-\kappa_b)}$ is of the same order of magnitude as $\sqrt{\langle v_{rh}^2\rangle/(1-\kappa_h)}$, because dark matter and baryons fall into the same potential well. Since thermal equilibrium implies $\frac{1}{2}m_p\langle v_{rb}^2\rangle = \frac{1}{2}m_h\langle v_{rh}^2\rangle$, we conclude that, unless $m_p(1-\kappa_b) \approx m_h(1-\kappa_h)$, dark matter is not in thermal equilibrium with baryons (mostly hydrogen atoms). So, on galactic scales, we can neglect dark matter-baryon interactions. If dark matter feels only the gravitational interaction, it can be shown that deviations of its trajectory due to particle-particle encounters, or interchange of energy with baryons, can be neglected on galactic scales. We also note that the ratio of dark matter to baryon densities in the galaxy is generally of the order of the universe average.

The galaxy density (21) reaches $\Omega_c\rho_{\text{crit}}$ at

$$r_{\max} = \left(\frac{\langle v_{rh}^2\rangle}{2\pi G\Omega_c\rho_{\text{crit}}}\right)^{1/2} \approx 6.6 \text{ Mpc}. \tag{37}$$

The age of the universe at, say, redshift $z = 6$, is 3×10^{16} s. In this time a particle with constant velocity 198 km/s reaches 0.2 Mpc, less than $r_{\max}$, and much farther than the last observed rotation velocity.

From (36), neglecting κ_h, we estimate that dark matter becomes non-relativistic at expansion parameter

$$a_{h\text{NR}} \equiv \frac{v_{h\text{rms}}(1)}{c} \approx 1.8\times 10^{-6}, \tag{38}$$

i.e. after e^+e^- annihilation, and while the universe is still dominated by radiation [3].

Now let us do the following back-of-the-envelope approximate calculations. An ultra-relativistic gas with zero chemical potential has a number density of particles $n(T) = 0.1218\cdot(kT/(\hbar c))^3(N_b + 3N_f/4)$ [3]. At expansion parameter a_{hNR} the temperature is $T_h(a_{h\text{NR}}) \approx m_h c^2/(3k)$. The present number density is $n(1) = n(a_{h\text{NR}})a_{h\text{NR}}^3 = \Omega_c\rho_{\text{crit}}/m_h$, if dark matter particles do not decay or annihilate at $\approx a_{h\text{NR}}$, *i.e.* if there is no "freeze-out". From these equations we obtain

$$m_h \approx \left(\frac{\Omega_c\rho_{\text{crit}}(3\hbar)^3}{0.1218\cdot v_{h\text{rms}}^3(1)}\right)^{1/4}(N_b + 3N_f/4)^{-1/4}, \tag{39}$$

or

$$\frac{m_h c^2}{e} \approx 107.3 \text{ eV}\left(\frac{760 \text{ m/s}}{v_{h\text{rms}}(1)}\right)^{3/4}(N_b + 3N_f/4)^{-1/4}. \tag{40}$$

For scalar dark matter, *i.e.* $N_b = 1$ and $N_f = 0$, and neglecting κ_h, we estimate the mass of the dark matter particles from (36): $m_h c^2/e \approx 140$ eV. At expansion parameter $a_{h\text{NR}}$ the photon temperature is $T_\gamma(a_{h\text{NR}}) = T_0/a_{h\text{NR}}$. From the preceding equations we obtain

$$\frac{T_h(a_{h\text{NR}})}{T_\gamma(a_{h\text{NR}})} \approx 0.386\left(\frac{v_{h\text{rms}}(1)}{760 \text{ m/s}}\right)^{1/4}(N_b + 3N_f/4)^{-1/4}, \tag{41}$$

or, for our example, $T_h(a_{h\mathrm{NR}})/T_\gamma(a_{h\mathrm{NR}}) \approx 0.354$. That this ratio is of order 1, given that the dark matter particle mass m_h is uncertain over 89 orders of magnitude [3], is surely telling us something! Furthermore, note that dark matter is sufficiently cooler than photons to (marginally) evade the "thermal relic" mass limits obtained from the Lyman-α forest [9], and sufficiently cool to not spoil the success of Big-Bang Nucleosynthesis [7]. Finally, within experimental uncertainties, dark matter is in thermal and diffusive equilibrium with the Standard Model sector, and decouples from this sector, at T somewhere between the top quark mass m_t and the temperature T_C of the deconfinement-confinement transition from quarks to hadrons (decoupling at a lower temperature compromises the agreement with Big Bang Nucleosynthesis [7]). For a proper treatment of the preceding estimates see [2] [10]. It turns out that Equations (40) and (41) change by less than 1%. For a summary of measurements and their interpretation, see [11]. For details of each measurement see the citations in [9].

Excersize to test the Boltzmann factor $\exp\left(-\Phi/(kT)\right) \approx \left(r_c/r\right)^2$: From the measured dark matter density in the vecinity of the sun [3], and other Milky Way data that you can find in the literature, estimate $v_{h\mathrm{rms}}(1)/\sqrt{1-\kappa_h}$. Is your answer consistent with (36)?

Exersizes: The isothermal assumption can be lifted by using the observed galaxy density runs $\rho_h(r)$ and $\rho_b(r)$ [12] [13]. Study these articles and obtain the adiabatic invariant $v_{h\mathrm{rms}}(1)/\sqrt{1-\kappa_h}$ from each of them. Are your answers consistent with (36)?

6. Galaxy Formation

Let us solve, by numerical integration, the following equations that describe the formation of a galaxy: Newton's equation

$$\nabla \cdot \boldsymbol{g} = -4\pi G\left(\rho_h + \rho_b\right), \tag{42}$$

the continuity equations

$$\frac{\partial \rho_h}{\partial t} = -\nabla \cdot \left(\boldsymbol{v}_h \rho_h\right), \tag{43}$$

$$\frac{\partial \rho_b}{\partial t} = -\nabla \cdot \left(\boldsymbol{v}_b \rho_b\right), \tag{44}$$

and Euler's equations

$$\frac{\mathrm{d}\boldsymbol{v}_h}{\mathrm{d}t} = \frac{\partial \boldsymbol{v}_h}{\partial t} + \left(\boldsymbol{v}_h \cdot \nabla\right)\boldsymbol{v}_h = \left(1-\kappa_h(t)\right)\boldsymbol{g} - \frac{1}{\rho_h}\nabla\left(\left\langle v_{rh}^2\right\rangle \rho_h\right), \tag{45}$$

$$\frac{\mathrm{d}\boldsymbol{v}_b}{\mathrm{d}t} = \frac{\partial \boldsymbol{v}_b}{\partial t} + \left(\boldsymbol{v}_b \cdot \nabla\right)\boldsymbol{v}_b = \left(1-\kappa_b(t)\right)\boldsymbol{g} - \frac{1}{\rho_b}\nabla\left(\left\langle v_{rb}^2\right\rangle \rho_b\right). \tag{46}$$

$\boldsymbol{g}(\boldsymbol{r},t)$ is the gravitation field, $\boldsymbol{r}$ is the proper (not comoving) coordinate vector, $\rho_h(\boldsymbol{r},t)$ and $\rho_b(\boldsymbol{r},t)$ are the mass densities, $\boldsymbol{v}_h(\boldsymbol{r},t)$ and $\boldsymbol{v}_b(\boldsymbol{r},t)$ are the velocity fields, and $\sqrt{\left\langle v_{rh}^2\right\rangle(t)}$ and $\sqrt{\left\langle v_{rb}^2\right\rangle(t)}$ are the radial (1-dimensional) velocity dispersions, *i.e.* thermal velocities, of dark matter and baryons (mostly

hydrogen), respectively. Equations (45) and (46) express the conservation of momentum. The static limits of Equations (42) - (46) are Equations (27) - (30). These equations need to be supplemented by the equations of state of dark matter and baryons at $r_{\min}$ in order to obtain a solution. The Maxwell distributions of baryons and dark matter have different temperatures $kT_b = m_p \langle v_{rb}^2 \rangle$ and $kT_h = m_h \langle v_{rh}^2 \rangle$, respectively. The dark matter velocity field converging onto the core has two consequences: it increases both the core density ρ_{0h} and temperature T_h, maintaining constant the dark matter adiabatic invariant (26) (as explained in lecture 2), and similarly for baryons. When the dark matter halo reaches a final stationary state its cored isothermal halo is defined by a single parameter ρ_{0h}.

An example, discussed in [15], is presented in **Figure 2**. For baryons we take $v_{brms}(1) = 21\,\text{m/s}$, corresponding to hydrogen decoupling from photons at $z \approx 150$ [16]. We set the initial $\rho_h(r)$ and $\rho_b(r)$ as shown in **Figure 2**. We integrate the equations in steps d*t*, and for each *t*, in steps d*r*, starting at $r_{\min}$, to calculate the new $\rho_b(r, t+\mathrm{d}t)$ and $\rho_h(r, t+\mathrm{d}t)$. The above equations need to be supplemented by the adiabatic conditions, so, for each step of *t*, we set, only once, *i.e.* for all *r*:

$$\sqrt{\langle v_{rh}^2 \rangle(t)} = \frac{v_{hrms}(1)}{\sqrt{3}} \left(\frac{\rho_h(r_{\min}, t)}{\Omega_c \rho_{\text{crit}}} \right)^{1/3}, \tag{47}$$

and

$$\sqrt{\langle v_{rb}^2 \rangle(t)} = \frac{v_{brms}(1)}{\sqrt{3}} \left(\frac{\rho_b(r_{\min}, t)}{\Omega_b \rho_{\text{crit}}} \right)^{1/3}. \tag{48}$$

Equation (47) is justified out to at least the last observed rotation velocity by the nearly flat rotation curves. The isothermal prescription (47) cannot be correct beyond $r_{\max}$ where the universe is expanding homogeneously. However, this is not a problem since, beyond $r_{\max}$, $\nabla(\langle v_{rh}^2 \rangle \rho_h)$ and $\nabla(\langle v_{rb}^2 \rangle \rho_b)$ are zero. While the hydrogen and helium gas remains adiabatic, *i.e.* until excitations, ionization, radiation, shocks and star formation become significant, we require (48). **Figure 2** illustrates the formation of a core, and how the galaxy reaches a stationary isothermal state starting from $r = 0$ and progressing outwards. For additional examples, see [14] and [15].

Note that, independently of the details of how the core reaches its final density ρ_{0h}, including spherical or filament collapse and galaxy mergers, this density fully specifies the cored isothermal sphere with its temperature, core radius, Boltzmann distribution, and adiabatic invariant $v_{hrms}(1)$ (up to a rotation, and perhaps also a relaxation, correction ≤ 1, that observationally is found to be in the approximate range 1 to 0.5 [6]).

Finally, let us mention that in the cold dark matter scenario, *i.e.* in the limit $\langle v_{rh}^2 \rangle \to 0$, we are left with no hydrostatic Equations (27) - (30), or hydrodynamical Equations (42) - (46).

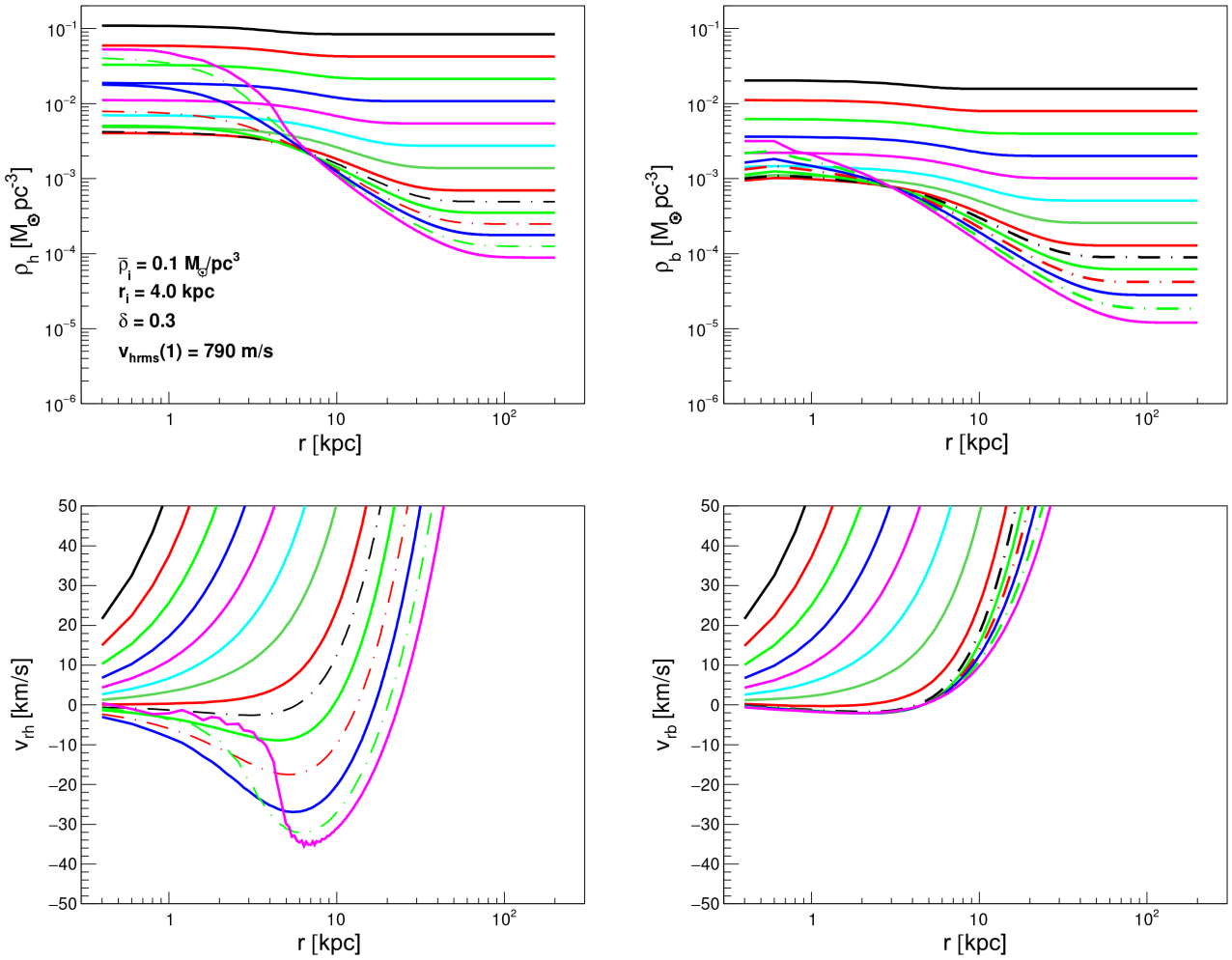

Figure 2. Shown is the formation of a warm dark matter plus baryon galaxy. The densities $\rho_h(r)$ and $\rho_b(r)$, and velocity fields $v_{rh}(r)$ and $v_{rb}(r)$, are presented at time-steps that increase by factors 1.4086 (or $\sqrt{1.4086}$ for the dot-dashed lines). The initial density perturbations are Gaussian, with parameters listed in the figure. In this example, dark matter is warm with $v_{hrms}(1) = 790$ m/s. $\kappa_h(t) = 0$. $\kappa_b(t)$ is increased from 10^{-4} to 1 keeping constant baryon angular momentum. Note the initial velocity field corresponding to the expansion of the universe. Note that both warm dark matter and baryons acquire cores. The baryon core is due to the baryon angular momentum conservation. The warm dark matter core is due to the adiabatic invariant feedback (47). Note the effect of this feedback on $v_{rh}(r)$ at the final times shown (studied in [14]). An isothermal steady state is reached for both warm dark matter and baryons, starting at $r = 0$ and then extending out to larger r, at least out to the observed rotation curves. This Figure is taken from [15].

7. Conclusions

We have studied galaxies, and galaxy formation, assuming that dark matter is warm. This scenario requires the addition of one parameter to the cold dark matter ΛCDM cosmology, namely the adiabatic invariant $v_{hrms}(1)$ defined in (4). We find that the formation of galaxies, all the way from linear perturbations in the early universe, until the galaxies reach an isothermal stationary state, conserves the adiabatic invariant $v_{hrms}(1)$ in the core to a good approximation. The arguments in favor of this view are not without objections, so observational validation is necessary. This adiabatic invariant feedback and the initial conditions

determine the final core density ρ_{0h}, and hence the entire cored isothermal sphere including its core radius and temperature (at least out to the observed spiral galaxy rotation curves). Note that it is not necessary to invoke dark matter self interactions, baryonic feedback, or fermionic dark matter quantum degeneracy, to justify a core (though these phenomena may influence the core). The observed spiral galaxy rotation curves allow measurements of $v_{hrms}(1)$ (up to a rotation, and perhaps also a relaxation, correction ≤ 1, that observationally is found to be in the approximate range 1 to 0.5 [6]). These measurements are consistent for galaxies with absolute luminosities spanning 3.5 orders of magnitude [6], so the analysis is validated by observations, and the interpretation that $v_{hrms}(1)$ is of cosmological origin is confirmed. Independent measurements of $v_{hrms}(1)$ are obtained by studying the consequences of the warm dark matter free-streaming suppression factor $\tau^2(k)$ of the cold dark matter power spectrum of density perturbations, *i.e.* galaxy stellar mass distributions, galaxy rest-frame ultra-violet luminosity distributions, first galaxies, and their effect on the reionization optical depth [17]. All of these measurements of $v_{hrms}(1)$ are consistent, solve the small scale problems of ΛCDM [18], and constrain the warm dark matter particle properties [9] [11] [19].

Conflicts of Interest

The author declares no conflicts of interest regarding the publication of this paper.

References

[1] Destri, C., de Vega, H.J. and Sanchez, N.G. (2013) *Physical Review D*, **88**, Article ID: 083512. https://doi.org/10.1103/PhysRevD.88.083512

[2] Paduroiu, S., Revaz, Y. and Pfenniger, D. (2015) Structure Formation in Warm Dark Matter Cosmologies Top-Bottom Upside-Down. https://arxiv.org/pdf/1506.03789.pdf

[3] Particle Data Group, Zyla, P.A., *et al.* (2020) *Progress of Theoretical and Experimental Physics*, **2020**, 083C01.

[4] Feynman, R.P., Leighton, R.B. and Sands, M. (1963) The Feynman Lectures on Physics. Vol. 1, Addison-Wesley Publishing Company, Reading, Mass.

[5] Lelli, F., McGaugh, S.S. and Schombert, J.M. (2016) *The Astronomical Journal*, **152**, 157. https://doi.org/10.3847/0004-6256/152/6/157

[6] Hoeneisen, B. (2022) *International Journal of Astronomy and Astrophysics*, **12**, 363-381. https://doi.org/10.4236/ijaa.2022.124021

[7] Hoeneisen, B. (2019) *International Journal of Astronomy and Astrophysics*, **9**, 71-96. https://doi.org/10.4236/ijaa.2019.92007

[8] Tonini, C., Lapi, A., Shankari, F. and Salucci, P. (2006) *The Astrophysical Journal*, **638**, L13-L16. https://doi.org/10.1086/500556

[9] Hoeneisen, B. (2023) Comparing Measurements and Limits on the Warm Dark Matter Temperature-to-Mass Ratio. arxiv: 2308.10356.

[10] Hoeneisen, B. (2022) *International Journal of Astronomy and Astrophysics*, **12**, 94-109. https://doi.org/10.4236/ijaa.2022.121006

[11] Hoeneisen, B. (2023) *European Journal of Applied Sciences*, **11**, 473-481. https://doi.org/10.18272/aci.v15i1.2961

[12] Karukes, E.V. and Salucci, P. (2017) *MNRAS*, **465**, 4703-4722. https://doi.org/10.1093/mnras/stw3055

[13] Borzou, A. (2021) *Journal of Cosmology and Astroparticle Physics*, **8**, 23. https://doi.org/10.1088/1475-7516/2021/08/023

[14] Hoeneisen, B. (2021) *International Journal of Astronomy and Astrophysics*, **11**, 489-508. https://doi.org/10.4236/ijaa.2021.114026

[15] Hoeneisen, B. (2022) *Journal of Modern Physics*, **13**, 932-948. https://doi.org/10.4236/jmp.2022.136053

[16] Weinberg, S. (2008) Cosmology. Oxford University Press, Oxford. https://doi.org/10.1093/oso/9780198526827.001.0001

[17] Hoeneisen, B. (2022) *International Journal of Astronomy and Astrophysics*, **12**, 258-272. https://doi.org/10.4236/ijaa.2022.123015

[18] Hoeneisen, B. (2023) *International Journal of Astronomy and Astrophysics*, **13**, 25-38. https://doi.org/10.4236/ijaa.2023.131002

[19] Hoeneisen, B. (2023) *International Journal of Astronomy and Astrophysics*, **13**, 217-235. https://doi.org/10.4236/ijaa.2023.133013